Nanoscale

Band gap reduction in van der Waals layered 2D materials via de-charge transfer mechanism

Journal:	*Nanoscale*
Manuscript ID	NR-ART-06-2018-004660.R1
Article Type:	Paper
Date Submitted by the Author:	18-Jul-2018

Complete List of Authors:	Zhang, Chunxiao; Xiangtan University, Laboratory for Quantum Engineering and Micro-Nano Energy Technology Huang, Huaqing; Department of Materials Science and Engineering, University of Utah Ni, Xiaojuan; ian University of Technology, Zhou, Yinong; Department of Materials Science and Engineering, University of Utah, Salt Lake City, UT 84112, United States of America Kang, Lei; Department of Materials Science and Engineering, University of Utah, Salt Lake City, UT 84112, United States of America Jiang, Wei; University of Utah, Materials Science & Engi. Chen, Haiyuan; University of Electronic Science and Technology of China, Research Branch of Functional Materials Zhong, Jianxin; Xiangtan University, Laboratory for Quantum Engineering and Micro-Nano Energy Technology Liu, Feng; University of Utah, Department of Materials Science

Band gap reduction in van der Waals layered 2D materials via de-charge transfer mechanism

Chunxiao Zhang,[ab] Huaqing Huang,[b] Xiaojuan Ni,[b] Yinong Zhou,[b] Lei Kang,[b] Wei Jiang,[b] Haiyuan Chen,[b] Jianxin Zhong,[*a] Feng Liu,[*bc]

A thickness dependent band gap is commonly found in layerd two-dimensional (2D) materials. Here, using C_3N bilayer as a prototypical model, we systematically investigate the evolution of band gap from single layer to bilayer using first principles calculation and tight binding modeling. We show that in addition to the widely known effect of interlayer hopping, de-charge transfer also plays an important role in tuning the band gap. The de-charge transfer is defined in reference to the charge states of atoms in the single layer without stacking, which shifts the energy level and modifies the band gap. Together with the band edge splitting induced by the interlayer hopping, the energy level shifting caused by the de-charge transfer determines the size of band gap in bilayer C_3N. Our finding, applicable to other 2D semiconductors, provides an alternative approach to realizing band gap engineering in 2D materials.

Introduction

Band gap is a fundamental parameter that governs the transport and light-matter interaction properties in condensed matter systems. For two-dimensional (2D) materials, constructing van der Waals layered structures is a practical route to tailor the electronic properties.[1–5] Along with other advances, such as the preserved ideal properties of isolated components[6–9] and gate-tunable band structure[10–15], the band gap is found to generally decrease and even undergoes a semiconductor-metal transition with the increasing thickness in van der Waals layered structures. This phenomenon is often attributed to the prevailing mechanism of energy splitting of band edge caused by the interlayer hopping in previous works[16–19]. However, this mechanism can be insufficient to explain the observed considerable band gap decreasing. Thus, there should be other hidden mechanism to also account for the overall band gap reduction.

Besides hopping, charge transfer is an important factor to modify the band gap as it causes the shifting of energy levels. Considering that in a hexagonal lattice with the same electronic energy at all the sites, as in graphene[20], a uniform π conjugation is formed, resulting in a semimetal with zero band gap. When introducing an electrostatic potential asymmetry (on-site energy difference) in the lattice, such as the case in BN and C_3N[21,22], the charge transfer will open a (charge) gap in proportion to this on-site energy (chemical potential) difference. Conversely, a de-charge transfer mechanism can be triggered by reducing/removing the site chemical potential difference, so that the gap will be decreased/closed. Here, we demonstrate that the de-charge transfer may ubiquitously at function to affect the band gap of van der Waals layered 2D compound materials.

We take C_3N[22,23] as an example to investigate the effect of de-charge transfer on its band gap using the first-principles calculation with the hybrid functional (HSE06) and a tight-binding (TB) model with the nearest-neighbor (NN) hopping. C_3N, as shown in Fig. (a), is a new promising 2D material with graphene-like honeycomb lattice. Single-layer C_3N has a medium band gap of about 1 eV in HSE level. Its band gap deceases sharply in bilayer and undergoes a semiconductor-metal transition when the number of layers is beyond three.[19] In this paper, we first show the dependence of band gap on charge transfer in the single layer, then give a general description of de-charge transfer and band gap reduction in the bilayer based on the TB model. Secondly, we demonstrate the effects of de-charge transfer on the band gap in the C_3N bilayer based on the Density functional theory (DFT) calculation and TB model.

Methods

First-principles calculations are performed based on the Kohn-Sham density functional theory (DFT)[24] using the Vienna ab initio simulation package (VASP)[25]. The generalized gradient approximation within the Perdew-Burke-Ernzerhof (PBE) functional form[26] is used for the exchange-correlation energy. To describe correctly van der Waals interactions within C_3N layers, a correction term (DFT-D2 method of Grimme[27]) is further added when calculating the conventional Kohn-Sham potential energy and interatomic forces. The DFT-D2 correction has been

[a]*Hunan Provincial Key Laboratory of Micro-Nano Energy Materials and Devices, Xiangtan University, Hunan 411105, People's Republic of China, Fax: +86732 58292468; Tel: +86732 52665818;E-mail:jxzhong@xtu.edu.cn*
[b]*Department of Materials Science and Engineering, University of Utah, Salt Lake City, UT 84112, United States of America E-mail:fliu@eng.utah.edu*
[c]*Collaborative Innovation Center of Quantum Matter, Beijing, 100084, People's Republic of China*

documented to well describe the graphite system[28] which is a structural analogue of the C_3N. A plane-wave cutoff of 600 eV is used to expand the valence electron wave functions. All atomic positions and lattice vectors are fully optimized by using a conjugate gradient algorithm to obtain the ground-state configuration. Atomic relaxation is performed until the change of total energy is smaller than 0.001 meV and the Hellmann-Feynman force on each atom is less than 0.005 eV/Å. A vacuum space of 20 Å is maintained in the z-axis to avoid mirror interactions. The Brillouin zone is represented by Monkhorst-Pack[29] special k-point mesh of $7\times7\times1$ for the geometry optimization and SCF computations. As the PBE functional is well known to underestimate the band gap, the more accurate HSE06 functional[30,31] is used to correct this underestimation.

Results and discussions

0.1 Tight-binding Model and Charge Transfer in C_3N single layer

We present the tight-binding model and parameters for C_3N single layer by fitting with the DFT bands in this section. Fig.1 (a) shows the optimized structure of C_3N single layer. The C_3N can be considered as that two carbon atoms are substituted by nitrogen atoms within P6/mmm symmetry in a 2×2 graphene supercell, and the lattice constant is shrunk from 4.92 Å to 4.86 Å. All carbon and nitrogen atoms are sp^2 hybridized, forming conjugated π bonds. The same length is found for C-C (1.403 Å) and C-N (1.403 Å) bonds. From band structures in Fig.1 (b), we find that the C_3N is a semiconductor with 1.04 eV of indirect band gap. The valence band maximum (VBM) locates at the M point and the conductance band minimum (CBM) locates at the Γ point, in agreement with previous results[19].

Since the bands near the Fermi level is dominated by the π conjugation, we employ a TB model involving the p_z-p_z interaction with the NN hopping to describe the C_3N single layer. The following eight-band model is used

$$H=\sum_i \varepsilon_C n_i+\sum_j \varepsilon_N n_j+\sum_{i\neq j} t^{||}c_i^{\dagger}c_j \tag{1}$$

where the summation runs over the lattice sites (six carbon sites and two nitrogen sites per unit cell). The ε_C and ε_N are the on-site energy at carbon and nitrogen sites, respectively. $t^{||}$ is the in-plane hopping parameter, and $c_i^{\dagger}(c_j)$ is the creation (annihilation) operator of electrons at site $i(j)$. Because we focus on the charge transfer caused by the on-site energy difference, the parameter $t^{||}$ is set to be 3.1 eV as in graphene[32,33]. We obtain the optimized on-site energy, ε_C=-2.6 and ε_N=-4.73, by fitting to the HSE bands as shown in Fig.1 (b). We note that the TB bands in Fig. 1b reproduce the most salient features of DFT bands, especially in terms of band gap size at the high-symmetry k-points. However, quantitatively there are notable differences between them. It is possible to significantly improve the TB bands to better agree with the DFT bands by adding up to 3NN hopping (see the supplementary information), but it will not affect the de-charge mechanism we discuss here. In comparison with graphene, one more band is occupied and the Dirac cone shifts below the Fermi level, since two more π electrons are present in the C_3N primitive cell than in the 2×2 graphene supercell. So that the Fermi level is located between the fifth and sixth band in our TB band structure.

To describe the charge transfer (Δe) in C_3N single layer, we calculate the electron density at each site based on the TB model. The TB Hamiltonian can operate in the space of coefficients of the TB functions $c(\vec{k})=(c_{N_1},c_{C_1},c_{C_2},c_{C_3},c_{C_4},c_{C_5},c_{C_6},c_{N_2})$ where $c_{C_i}=c_{C_i}(\vec{k})$ and $c_{N_i}=c_{N_i}(\vec{k})$ are the coefficients for C and N atoms, respectively. The total eigenfunction of the system is then given by

$$\Psi=\sum_{i=1}^{6} c_{C_i}\psi_{\vec{k}}^{C_i}(\vec{r})+\sum_{j=1}^{2} c_{N_j}\psi_{\vec{k}}^{N_j}(\vec{r}) \tag{2}$$

The eight coefficients in Eq. (2), for fixed value of $t^{||}$, can be obtained by diagonalizing Hamiltonian matrix. Based on the coefficients, the electronic density at each carbon and nitrogen site is given by

$$n_{C_i}=\sum_{n=1}^{N_b}\int\int |c_{n,C_i}|^2 \mathrm{d}k_x\mathrm{d}k_y \tag{3}$$

$$n_{N_j}=\sum_{n=1}^{N_b}\int\int |c_{n,N_j}|^2 \mathrm{d}k_x\mathrm{d}k_y \tag{4}$$

where N_b is the number of occupied bands and N_b = 5 in C_3N single layer. The charge transfer is determined to be the variation of electron density at nitrogen site as follows

$$\Delta e=n_{N_j}-n_0 \tag{5}$$

where n_0 is the electron density at each site in a system with electrostatic potential symmetry, *i.e.*, the on-site energies are equal at all the sites and the π electrons uniformly distribute in the single layer with n_0 = 1.25 e at each site.

In Fig.1 (c) we show the dependence of the Δe and band gap on the on-site energy difference ($\Delta\varepsilon=\varepsilon_C-\varepsilon_N$) with the ε_C being fixed to be -2.6 eV. The origin point is corresponding to the system with electrostatic potential symmetry. From Fig.1 (c), one can see that both the Δe and band gap increases with the $\Delta\varepsilon$. The on-site energy difference induces the charge transfer from carbon to nitrogen site, which shifts the energy levels near the Fermi level and then opens a band gap. The stars indicate the charge transfer and band gap in C_3N single layer where 0.34 e of electrons transfer into each nitrogen site. From *bader* charge analysis[34] based on the DFT calculation, we find 0.4 electrons transfer into the p_z state of each nitrogen atom in reasonably good agreement with the TB estimation.

0.2 General description for band gap reduction and de-charge transfer in the bilayer

A simplified TB model is used to give a general description for the band gap and de-charge transfer in van der Waals bilayer. Based on the first-principles energy calculation, the AD stacking

as shown in Fig.2 (a) is the most stable C_3N bilayer (The stability of C_3N bilayer is discussed in details in the supplementary information). In AD stacking, the top layer is directly stacked on the bottom layer, but the top layer of atoms are shifted by a half primitive cell along the armchair direction. The inter-layer spacing is 3.175 Å, corresponding to the van der Waals interaction. In the TB model, the bilayer is modeled as two coupled single-layer C_3N hexagonal lattices with additional inter-layer hopping, arranged according to AD stacking. For simplicity, the NN inter-layer hopping is considered with equal magnitude, which is qualitatively good enough for now. The TB Hamiltonian reads

$$H = \sum_i \varepsilon_C n_i + \sum_j \varepsilon_N n_j + \sum_{i \neq j} t^{\|} c_i^{\dagger} c_j + \sum_{i \neq j} \gamma c_i^{\dagger} c_j \quad (6)$$

where the first three items have the same meaning as in Eq. (1), while the forth item describes the inter-layer interaction. Fig.2 (b) shows the evolution of band gap as functions of both inter-layer hopping (γ) and in-plane on-site energy difference ($\Delta\varepsilon$). We find that either increasing γ or decreasing $\Delta\varepsilon$ is able to reduce the band gap. For example, keeping $\Delta\varepsilon$ to be 2.13 eV as the value in C_3N single layer the band gap is closed by increasing the inter-layer hopping to γ =0.54 eV, while neglecting the inter-layer hopping the band gap would be closed without on-site energy difference.

The electron densities of individual atoms are obtained by Eq. (3) and (4) with N_b=10. The amount of de-charge transfer is also determined by calculating the change of electrons at each nitrogen site:

$$\Delta e = n_N - n_{N_j} \quad (7)$$

where n_N is the electron density of the nitrogen site in the C_3N single layer which is 1.59 e as obtained by Eq. (4) with N_b=5. n_{N_j} is the electron density of each nitrogen site in the bilayer. Because both γ and $\Delta\varepsilon$ can modify the band gap, we study the dependence of de-charge transfer on γ and $\Delta\varepsilon$, respectively. As shown in Fig.3 (a), the de-charge transfer is almost independent of γ. For instance, when increasing the γ from 0 eV to 0.4 eV and keeping $\Delta\varepsilon$ at 1.63 eV, the de-charge transfer only changes from 0.050 e to 0.057 e, but the band gap significantly decreases from 0.807 eV to 0.022 eV. On the other hand, the de-charge transfer is almost linearly increasing with $\Delta\varepsilon$. For instance, keeping γ at 0.3 eV, 0.072 e of de-charge transfer occurs from N to C and the band gap is reduced from 0.457 eV to 0.12 eV, when $\Delta\varepsilon$ is decreased from 2.13 eV to 1.43 eV, as shown in Fig.3 (b). In general, we find that inter-layer hopping reduces the band gap by inducing energy splitting of band edges while de-charge transfer reduces the band gap by shifting the energy level near the Fermi level.

0.3 The mechanism of thickness dependent band gap tuning in C_3N bilayer

In this section, we illustrate the effects of de-charge transfer on the thickness dependent band gap of C_3N bilayer based on both DFT calculation and TB modeling in details. To describe the de-charge transfer in C_3N bilayer based on the DFT calculation, we analyze the redistribution of charge density ($\Delta\rho_e$) which is determined as follows

$$\Delta\rho_e = \rho_{bilayer} - 2\rho_{monolayer} \quad (8)$$

where $\rho_{bilayer}$ and $\rho_{monolayer}$ are the charge density of C_3N bilayer and isolated C_3N single layer, respectively. The distribution of $\Delta\rho_e$ is shown in Fig.4 (a). One can see that the distribution of $\Delta\rho_e$ is symmetric between the two layers. A depletion of charge density is found in the p_z state of nitrogen and its neighboring carbon atoms in the armchair direction, while a accumulation of the charge density is found in the p_z state of other carbon atoms. The charge mainly transfers back from nitrogen atoms with high electron negativity to carbon atoms with low electron negativity in the zigzag direction, which manifests the de-charge transfer. The evolution of the de-charge transfer with inter-layer spacing is shown in Fig.4 (b). We find that when the interlayer spacing is enlarged by 1.2 Å relative to the C_3N bilayer, the interlayer interaction becomes so weak that each layer could be consider as an isolated single layer. In that case, the band gap is almost equal to that of C_3N single layer and the de-charge transfer is close to zero. Reducing the interlayer spacing gives rise to the inter-layer interaction which results in both band gap reduction and de-charge transfer. For instance, the band gap is reduced to 0.89 eV while 0.031 e of electrons transfer out of each N-p_z (calculated based on the *bader* charge analysis) when the inter-layer spacing decreases to 3.175 Å.

Finally, we further clarify the mechanism of thickness dependent band gap based on TB model. From the distribution of charge density and the electron density at individual site, we introduce different on-site energies at two non-equivalent carbon sites (C_1 and C_2) in each layer, as well as two different interlayer hoppings (C-N interlayer hopping γ_1 and C-C interlayer hopping γ_2) as shown in Fig.5 (a). The band structure of C_3N is shown in Fig.5 (b). From the HSE band structures, we find that the degeneracy between K_1 and K_2 (M_1 and M_2) is removed because of the broken of the inversion symmetry in comparison with C_3N single layer. The C_3N bilayer is also an indirect semiconductor with the VBM and CBM locating at M_2 and Γ, respectively, but the band gap decreases from 1.04 eV to 0.089 eV. Fitting the TB bands to the HSE results, we find that the energy splitting near the Fermi level mainly originates from the interlayer hopping. By fitting the energy splitting to the DFT results at the band edges, the γ_1 and γ_2 are obtained to be 0.42 eV and 0.3 eV, respectively. If keeping all the on-site energies as the values in the C_3N single layer, when the γ_1 and γ_2 are set to be 0.42 eV and 0.3 eV, the band gap decreases from 1.04 eV to 0.336 eV but the de-charge transfer is just 0.002 e comparing with the C_3N single layer. It indicates that the interlayer hopping is indeed an important factor to tune the band gap but has little effect on the de-charge transfer. The 0.336 eV of band gap is still much larger than the DFT band gap (0.089 eV in HSE level) of C_3N bilayer. In order to fit the band gap with the DFT result, the on-site energies are then modified to -4.33 eV, -2.50 eV and -2.60 eV at the N, C_1 and C_2 sites, respectively. Based on these TB parameters, the de-charge transfer is calculated to be 0.036 e by Eq. (7), which agrees with the result of the *bader* charge analysis. So that de-charge

transfer induces about 0.247 eV additional band gap reduction. Consequently, in the C_3N bilayer the inter-layer interaction not only induces the inter-layer hopping but also changes the in-plane on-site energy. The variation of in-plane on-site energy difference causes the de-charge transfer which shifts the energy level near the Fermi level. Together with energy splitting induced by interlayer hopping, de-charge transfer is another important parameter to tune the band gap.

Conclusion

we propose that de-charge transfer provides an important mechanism for band engineering of van der Waals layered 2D materials, in addition to interlayer hopping. We reveal this mechanism by a systematic study of band gap of C_3N bilayer as a model system using first principles calculations and tight-binding modeling. We believe this mechanism is generally applicable to all the 2D semiconductor homo- and hetero-junctions. Our findings will be not only fundamentally useful to better understand the band gap evolution of 2D materials as a function of thickness, but also practically significant for band gap engineering of 2D materials.

References

1 H. Wang, L. Yu, Y.-H. Lee, Y. Shi, A. Hsu, M. L. Chin, L.-J. Li, M. Dubey, J. Kong and T. Palacios, *Nano Letters*, 2012, **12**, 4674–4680.

2 C.-J. Shih, Q. H. Wang, Y. Son, Z. Jin, D. Blankschtein and M. S. Strano, *ACS Nano*, 2014, **8**, 5790–5798.

3 Y. Deng, Z. Luo, N. J. Conrad, H. Liu, Y. Gong, S. Najmaei, P. M. Ajayan, J. Lou, X. Xu and P. D. Ye, *ACS Nano*, 2014, **8**, 8292–8299.

4 M. Bernardi, M. Palummo and J. C. Grossman, *Nano Letters*, 2013, **13**, 3664–3670.

5 M. M. Furchi, A. Pospischil, F. Libisch, J. Burgdorfer and T. Mueller, *Nano Letters*, 2014, **14**, 4785–4791.

6 G. Gao, W. Gao, E. Cannuccia, J. Taha-Tijerina, L. Balicas, A. Mathkar, T. N. Narayanan, Z. Liu, B. K. Gupta, J. Peng, Y. Yin, A. Rubio and P. M. Ajayan, *Nano Letters*, 2012, **12**, 3518–3525.

7 A. K. Geim and I. V. Grigorieva, *Nature*, 2013, **499**, 419.

8 J. E. Padilha, A. Fazzio and A. J. R. da Silva, *Phys. Rev. Lett.*, 2015, **114**, 066803.

9 W. Xia, L. Dai, P. Yu, X. Tong, W. Song, G. Zhang and Z. Wang, *nanoscale*, 2017, **9**, 4324.

10 J. Oostinga, H. Heersche, X. Liu, A. F. Morpurgo and L. M. K. Vandersypen, *Nature Materials*, 2007, **7**, 151.

11 T. Ohta, A. Bostwick, T. Seyller, K. Horn and E. Rotenberg, *Science*, 2006, **313**, 951–954.

12 A. Ramasubramaniam, D. Naveh and E. Towe, *Phys. Rev. B*, 2011, **84**, 205325.

13 M. Kang, B. Kim, S. H. Ryu, S. W. Jung, J. Kim, L. Moreschini, C. Jozwiak, E. Rotenberg, A. Bostwick and K. S. Kim, *Nano Letters*, 2017, **17**, 1610–1615.

14 Y. Liu, Z. Qiu, A. Carvalho, Y. Bao, H. Xu, S. J. R. Tan, W. Liu, A. H. Castro Neto, K. P. Loh and J. Lu, *Nano Letters*, 2017, **17**, 1970–1977.

15 B. Deng, V. Tran, Y. Xie, H. Jiang, C. Li, Q. Guo, X. Wang, H. Tian, S. J. Koester, H. Wang, J. J. Cha, Q. Xia, L. Yang and F. Xia, *Nature Communications*, 2017, **8**, 14474.

16 T. Cheiwchanchamnangij and W. R. L. Lambrecht, *Phys. Rev. B*, 2012, **85**, 205302.

17 Z. Zhu and D. Tománek, *Phys. Rev. Lett.*, 2014, **112**, 176802.

18 J. Qiao, X. Kong, Z.-X. Hu, F. Yang and W. Ji, *Nature Communications*, 2014, **5**, 4475.

19 W. Li, X. Dai, J. Morrone, G. Zhang and R. Zhou, *nanoscale*, 2017, **9**, 12025.

20 K. S. Novoselov, A. K. Geim, S. V. Morozov, D. Jiang, M. I. Katsnelson, I. V. Grigorieva, S. V. Dubonos and A. A. Firsov, *Nature*, 2005, **438**, 197.

21 K. Watanabe, T. Taniguchi, H. Kanda, D. Jiang, M. I. Katsnelson, I. V. Grigorieva, S. V. Dubonos and A. A. Firsov, *Nature Materials*, 2004, **3**, 404.

22 J. Mahmood, E. K. Lee, M. Jung, D. Shin, H.-J. Choi, J.-M. Seo, S.-M. Jung, D. Kim, F. Li, M. S. Lah, N. Park, H.-J. Shin, J. H. Oh and J.-B. Baek, *Proceedings of the National Academy of Sciences*, 2016, **113**, 7414–7419.

23 S. Yang, W. Li, C. Ye, G. Wang, H. Tian, C. Zhu, P. He, G. Ding, X. Xie, Y. Liu, Y. Lifshitz, S. Lee, Z. Kang and M. Jiang, *Advanced Materials*, **29**, 1605625.

24 W. Kohn and L. J. Sham, *Phys. Rev.*, 1965, **140**, A1133–A1138.

25 G. Kresse and J. Furthmĺźller, *Computational Materials Science*, 1996, **6**, 15 – 50.

26 J. P. Perdew, K. Burke and M. Ernzerhof, *Phys. Rev. Lett.*, 1996, **77**, 3865–3868.

27 G. Stefan, *Journal of Computational Chemistry*, **27**, 1787–1799.

28 X. Chen, F. Tian, C. Persson, W. Duan and N.-x. Chen, *Scientific Reports*, 2013, **3**, 3046.

29 H. J. Monkhorst and J. D. Pack, *Phys. Rev. B*, 1976, **13**, 5188–5192.

30 J. Heyd, G. E. Scuseria and M. Ernzerhof, *The Journal of Chemical Physics*, 2003, **118**, 8207–8215.

31 A. V. Krukau, O. A. Vydrov, A. F. Izmaylov and G. E. Scuseria, *The Journal of Chemical Physics*, 2006, **125**, 224106.

32 P. Gava, M. Lazzeri, A. M. Saitta and F. Mauri, *Phys. Rev. B*, 2009, **79**, 165431.

33 A. A. Avetisyan, B. Partoens and F. M. Peeters, *Phys. Rev. B*, 2009, **80**, 195401.

34 W. Tang, E. Sanville and G. Henkelman, *Journal of Physics: Condensed Matter*, 2009, **21**, 084204.

Acknowledgments

This work is supported by National Natural Science Foundation of China (Grant No. 11474244), the Program for Chang Jiang Scholars and Innovative Research Team in University(IRT13093), Natural Science Foundation of Hunan Province of China (Grant No. 2016JJ3118). H. H., X. N., N. Z., F. L. is supported by

U.S. DOE-BES (Grant No. DE-FG02-04ER46148). We also acknowledge financial support from China Scholarship Council. The calculations were partly done on the CHPC at the University of Utah, United States of America.

Graphics and tables

Graphics

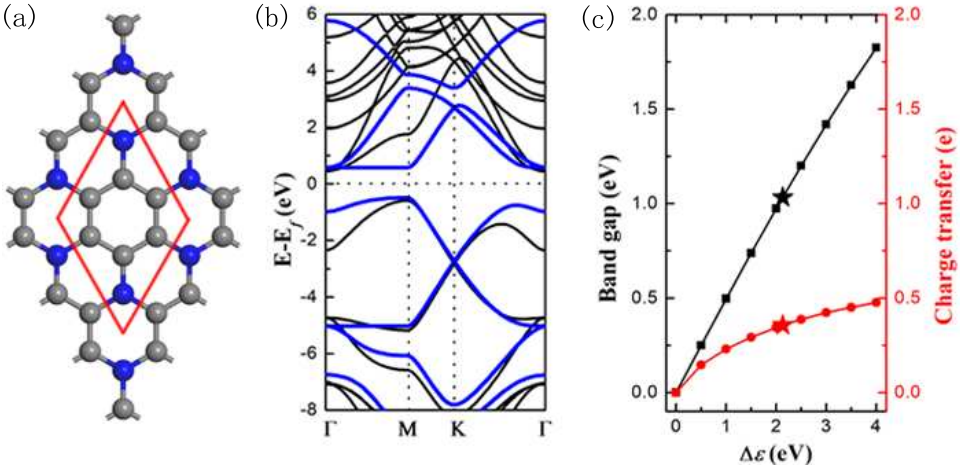

Fig. 1 (color online) (a) Top view of the crystal structure of monolayer C_3N. Red dashed lines indicates the primitive cell. (b) Tight-binding fitting (blue-solid lines) of the HSE bands (black-solid lines) for monolayer C_3N. Tight-binding fitting was made for the p_z bands with the NN hopping. (c) The evolution of band gap and charge transfer with $\Delta\varepsilon$ based on the tight-binding simulation. Black and red curves represent band gap and charge transfer, respectively.

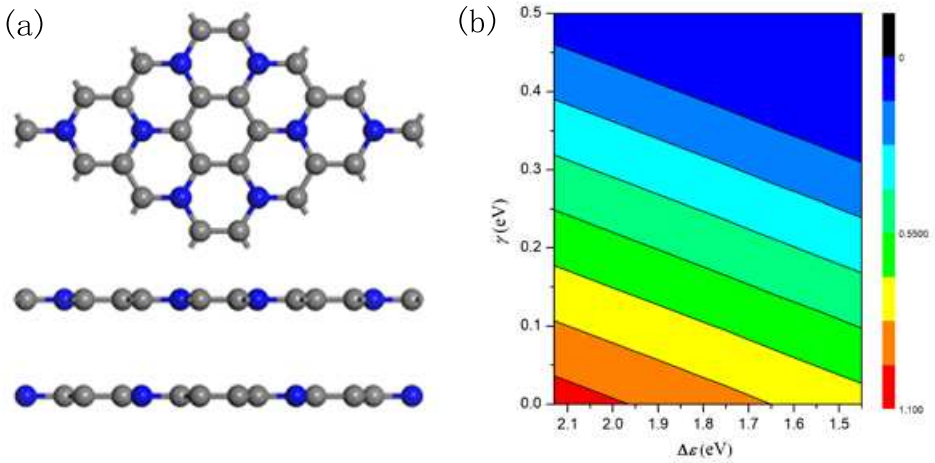

Fig. 2 (color online) (a) Top and side view of the crystal structure of AD-stacked C_3N bilayer. Blue and gray ball represent nitrogen and carbon atoms, respectively. (b) Evolution of band gap with both γ and $\Delta\varepsilon$.

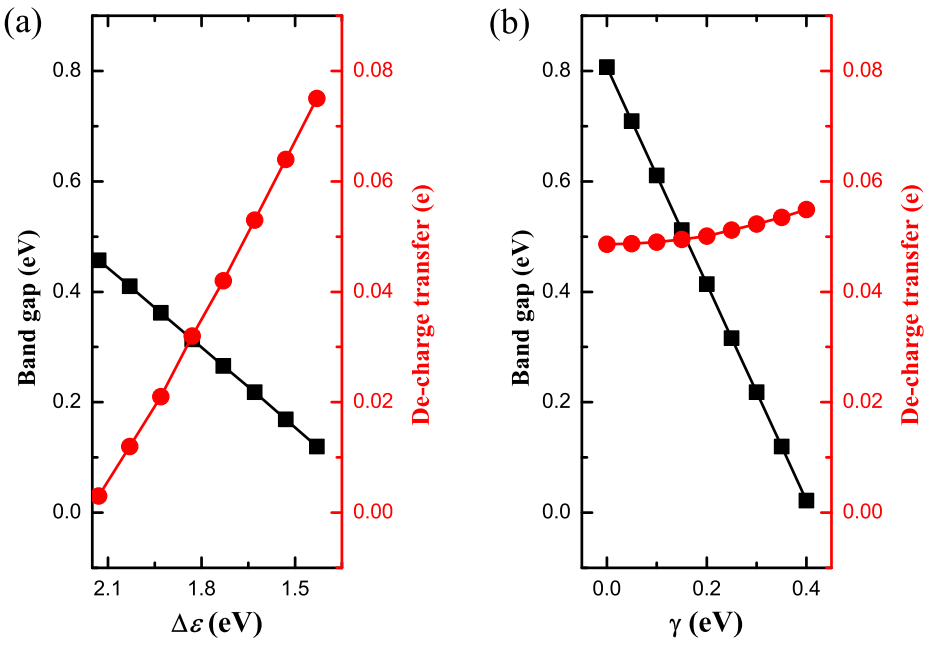

Fig. 3 (color online) (a) The dependence of both de-charge transfer and band gap on the γ when $\Delta\varepsilon^{\|}$ = 1.63 eV. (b) The dependence of both de-charge transfer and band gap on the $\Delta\varepsilon^{\|}$ when γ = 0.3 eV. Black and red curves represent band gap and de-charge transfer, respectively.

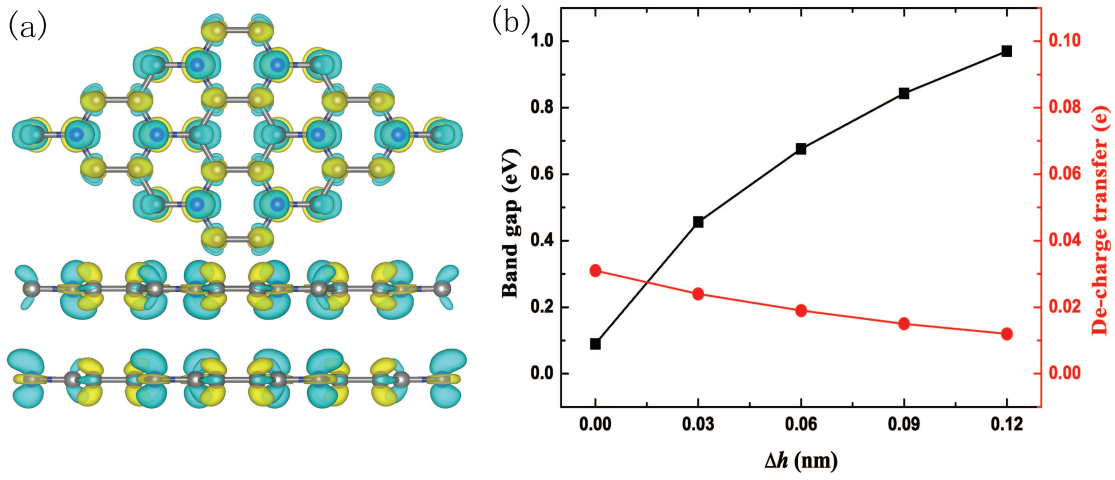

Fig. 4 (color online) (a) The redistribution of charge density in bilayer C_3N. Blue and yellow isosurfaces correspond to positive and negative values of 2×10^{-3} e/Å. (b) The dependence of the band gap and de-charge transfer on the interlayer spacing. The de-charge transfer is calculated based on the *bader* charge analysis and Δh is the variation of interlayer spacing relative to the C_3N bilayer.

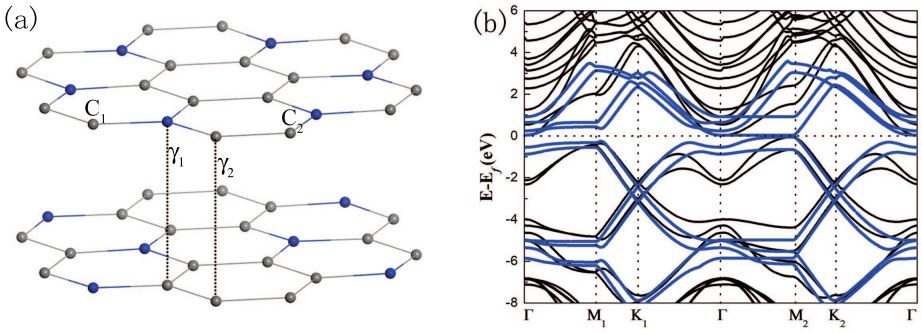

Fig. 5 (color online) (a) Schematic of the bilayer lattice containing two nonequivalence carbon site and two different interlayer hopping in the unit cell. (b) Tight-binding fitting (blue-solid lines) of the HSE bands (black-solid lines) for bilayer C_3N. Tight-binding fitting was made for the p_z bands within NN hopping. The difference of interlayer hopping and on-site energy of nonequivalent carbon sites are considered.